and at the Flory Θ temperature, after normalization of the appropriate time scale by $\tau_C = \eta_0 R_0^{(s)}$.

Acknowledgment. This study, which was supported in part by a grant from the Polymers Program, Division of Materials Science, National Science Foundation, comprises part of the Ph.D. dissertation of J.O.P.

Registry No. Polystyrene, 9003-53-6.

References and Notes

(1) Berry, G. C. *J. Chem. Phys.* **1967**, *46*, 1338.
(2) Hager, B. L.; Berry, G. C. *J. Polym. Sci., Polym. Phys. Ed.* **1982**, *20*, 211.
(3) Berry, G. C.; Fox, T. G *Adv. Polym. Sci.* **1968**, *5*, 261.
(4) Grasseley, W. W. *Adv. Polym. Sci.* **1974**, *16*, 1.
(5) Casassa, E. F.; Berry, G. C. In *Comprehensive Polymer Science*; Booth, C., Price, C. Eds.; Pergamon Press: Oxford, 1988; Vol. 2, Chapter 3.
(6) Daoud, M.; Cotton, J. P.; Farnoux, B.; Jannink, G.; Sarma, G.; Benoit, H.; Duplessix, R.; Picot, C.; de Gennes, P.-G. *Macromolecules* **1975**, *8*, 804.
(7) Berry, G. C. In *Encyclopedia of Polymers Science and Engineering*; Mark, H., Overberger, C. G., et al., Eds.; Wiley: New York, 1987; Vol. 8, p 721.
(8) Muthukumar, M.; Edwards, S. F. *Polymer* **1982**, *23*, 345.
(9) Doi, M.; Edwards, S. F. *The Theory of Polymer Dynamics*; Clarendon Press: Oxford, 1987; Chapter 7.
(10) Doi, M. *J. Polym. Sci., Polym. Phys. Ed.* **1983**, *21*, 667.
(11) Nakamura, K.; Wong, C.-P.; Berry, G. C. *J. Polym. Sci., Polym. Phys. Ed.* **1984**, *22*, 1119.
(12) Bernstein, B.; Kearsley, E. A.; Zappas, L. J. *Trans. Soc. Rheol.* **1963**, *7*, 391.
(13) Ferry, J. D. *Viscoelastic Properties of Polymers*, 3rd. ed.; Wiley: New York, 1980; Chapter 1.
(14) Riande, E.; Markovitz, H.; Plazek, D. J.; Raghupathi, N. *J. Polym. Sci., Symp. No. 50* **1975**, 405.
(15) Fox, T. G; Loshaek, S. *J. Polym. Sci.* **1955**, *15*, 371.
(16) Berry, G. C.; Birnboim, M. H.; Park, J. O.; Meitz, D. W.; Plazek, D. J. *J. Polym. Sci., Part B*, in press.
(17) Birnboim, M. H.; Burke, J. S.; Anderson, R. L. In *Proc. Fifth Int. Congr. Rheol.*; Onogi, S., Ed.; University of Tokyo Press: Tokyo, 1969; Vol. 1, p 409.
(18) Riande, E.; Markovitz, H. *J. Polym. Sci., Polym. Phys. Ed.* **1975**, *13*, 947.
(19) Berry, G. C.; Plazek, D. J. In *Glass: Science and Technology*; Uhlmann, D. R., Kreidl, N. J., Eds.; Academic Press: New York, 1986; Chapter 6.
(20) Markovitz, H. In *Physics Vade Mecum*; Anderson, H. L., Ed.; Institute of Physics: New York; p 274.
(21) Plazek, D. J.; Riande, E.; Markovitz, H.; Raghupathi, N. *J. Polym. Sci., Polym. Phys. Ed.* **1979**, *17*, 2189.
(22) Plazek, D. J., private communication.
(23) (a) Takahashi, Y.; Noda, I.; Nagasawa, M. *Macromolecules* **1985**, *18*, 2220. (b) Takahashi, Y.; Umeda, M.; Noda, I. *Macromolecules* **1988**, *21*, 2257.
(24) Cox, W. P.; Merz, B. H. *J. Polym. Sci.* **1958**, *28*, 619.
(25) Kusamizu, S.; Holmes, L. A.; Moore, A. A.; Ferry, J. D. *Trans. Soc. Rheol.* **1968**, *12*, 559.
(26) Einaga, Y.; Osaki, K.; Kurata, M.; Tamura, M. *Macromolecules* **1971**, *4*, 87.
(27) de Gennes, P.-G. *Scaling Concepts in Polymer Physics*; Cornell University Press: Ithaca, NY, 1979; Chapter 8.
(28) Yamakawa, H. *Modern Theory of Polymer Solutions*; Harper & Row: New York, 1971; Chapter 7.
(29) Kulicke, W.-M.; Kniewske, R. *Rheol. Acta* **1984**, *23*, 75.
(30) Bueche, B. *Physical Properties of Polymers*: Interscience: New York, 1962; Chapter 5.
(31) Park, J. O. Ph.D. Thesis, Carnegie-Mellon University, 1986.
(32) Venkatraman, S.; Berry, G. C.; Einaga, Y. *J. Polym. Sci., Polym. Phys. Ed.* **1985**, *23*, 1275.

Solvation Effect upon Glass Transition Temperature and Conductivity of Poly(ethylene oxide) Complexed with Alkali Thiocyanates

S. Besner and J. Prud'homme*

Department of Chemistry, University of Montreal, Montreal, Quebec, Canada H3C 3V1.
Received July 26, 1988; Revised Manuscript Received December 12, 1988

ABSTRACT: The apparent solvation numbers, SN, of LiSCN, KSCN, and CsSCN in amorphous poly(ethylene oxide) (PEO) have been inferred from the salt saturation concentrations in melt-quenched amorphous mixtures. On an EO unit molar basis, these numbers are EO/Li = 3, EO/K = 4.9, and EO/Cs = 9. They increase linearly with the cation atomic surfaces and, when extrapolated to zero atomic surface value, they yield an apparent solvation number of 2 for the thiocyanate anions. In turn, the apparent coordination numbers, CN, of the alkali cations with respect to the EO units are given by the relation CN = SN − 2. The glass transition temperature (T_g) dependence upon the salt molar concentration is the same for the three systems, suggesting that the cation–EO binding energy is inversely proportional to CN. More surprising is that for the molar ratio EO/M = 8, for which the ac conductivity of amorphous mixtures of the three systems could be investigated in the temperature range 10–100 °C, conductivity magnitude at reduced temperatures $T - T_g$ is directly proportional to CN. This straightforward correlation is interpreted in terms of an ionic structure in the concentrated regime that would consist of ions surrounded by an ion atmosphere of opposite sign. Conduction appears to occur through an exchange of solvating EO units at a rate determined by both the segmental motion of the PEO chains and the cation–EO binding energy. Ion–ion interactions are also important as judged by a decrease of conductivity magnitude with increasing salt concentration for the PEO–LiSCN system.

Introduction

In a recent paper,[1] we reported a complete phase diagram for the PEO–NaSCN system (PEO = poly(ethylene oxide)) together with a partial phase diagram for the PEO–KSCN system. In each case the phase diagram was constructed by means of DSC measurements performed on solvent-cast mixtures prepared with a low molecular weight PEO sample ($M_n = 4 \times 10^3$), in order to avoid entanglement effect upon crystallinity. In spite of this concern, it turned out that only the mixtures with NaSCN were highly crystalline over the entire composition range. Those with KSCN exhibited a crystallinity gap in the range of the PEO-rich compositions. The phase diagrams of the PEO–NaSCN and PEO–KSCN systems show great similarities. Each involves an intermediate crystalline compound, $P(EO_3{\cdot}NaSCN)$ or $P(EO_{\sim 4}{\cdot}KSCN)$, that melts incongruently (at 182 or 95 °C) to yield the solid salt. Above the melting temperature of the intermediate compound, the solubility curve of each salt is nearly vertical. Also, in each case the same solubility limit as that defined

0024-9297/89/2222-3029$01.50/0

at temperatures above the melting point of the intermediate compound is indicated at considerably lower temperatures by the composition dependence of T_g for melt-quenched mixtures. This temperature-independent behavior of salt solubility has been interpreted in terms of a solvation reaction taking place in liquid or amorphous PEO. According to this interpretation, on an EO unit molar basis, salt solubility would be governed by the following equilibria[1]

$$\text{salt}_S \rightleftharpoons \text{salt}_L \quad (1)$$

$$n\text{EO}_L + \text{salt}_L \rightleftharpoons \text{EO}_n\cdot\text{salt}_L \quad (2)$$

where S and L denote solid and liquid phases, respectively.

The solvation reaction (2) proceeds with an important decrease of free enthalpy (large equilibrium constant) that favors its completion over a large domain of temperatures. Therefore, over this range, dissolution through reaction 1 is entirely controlled by the solvation reaction 2 and the solution concentration at saturation corresponds to the solvate composition. Note that this thermodynamical model does not assume any particular structure for the solvate except a well-defined stoichiometry. According to the solubility data reported in the previous paper,[1] this stoichiometry corresponds to EO/Na = 4 for NaSCN and EO/K = 4.9 for KSCN. The important feature of this dissolution–solvation scheme is a decrease of free enthalpy for the solvation reaction (2) that is substantial enough to compensate for the increase of free enthalpy associated with the dissolution reaction (1). In other words, saturation is not imposed by the magnitude of the lattice energy of the salt but by the intrinsic capacity of PEO for complexing the salt. The more convincing argument for this feature is the finite solubility of both NaSCN and KSCN even at temperatures above their melting points.[1] For instance, in the case of KSCN whose melting point at 176 °C is moderate enough to prevent any significant thermal decomposition of the polymer, a solubility limit corresponding to EO/K = 4.1 is indicated at this temperature. Also, saturation by liquid KSCN at temperatures above 176 °C is observed by visual inspection upon heating vacuum-sealed tubes containing mixtures with EO/K less than 4.

For better comprehension of the physical parameters governing alkali thiocyanate solubility in liquid PEO, we have examined the PEO–LiSCN and the PEO–CsSCN systems which contain alkali metal cations with a wider range of atomic sizes. LiSCN is considerably more hygroscopic than the other alkali thiocyanates and serious difficulties were encountered for preparing moisture-free solvent-cast mixtures with this salt. Nevertheless, from DSC measurements carried out on mixtures dried under vacuum at 125 °C, it has been possible to define some general features for the PEO–LiSCN system. Like the PEO–KSCN system, it presents an important crystallinity gap in the range of the PEO-rich compositions that prevents the utilization of calorimetric data for an accurate determination of the stoichiometry of its intermediate compound. This compound melts incongruently at 138 °C and its approximate formula is $P(EO_{\sim 2}\cdot LiSCN)$. On the other hand, contrary to the other systems, the PEO–CsSCN system yields amorphous mixtures saturated by either the salt or the crystalline PEO component.

The present paper is devoted to the glass transition behavior of melt-quenched mixtures of the four PEO–alkali thiocyanate systems. This subject is important because it appears that ionic conduction in amorphous PEO and similar polymers is governed by the glass transition temperature, T_g, of the mixture and that, in turn, T_g is dependent upon the salt concentration.[2-4] This latter dependence is examined in detail for the four alkali thiocyanates in the concentration domains where the quenched mixtures yield completely amorphous materials. The T_g data allow the characterization of an apparent solvation number, SN, for each salt except NaSCN. Also examined is the conductivity σ of EO/M = 8 amorphous mixtures with each salt (except NaSCN) over the temperature range 10–100 °C. An analysis of the data made in terms of the variables SN and T_g reveals a clear correlation between σ and SN that provides some clarifications concerning the conduction mechanism in amorphous polymer electrolytes.

Since the PEO–CsSCN system is unique among the present systems by its lack of a crystalline compound, it has been examined in more detail. Its complete phase diagram is presented at the beginning of this paper. It is shown that PEO crystallization in the PEO–CsSCN system does not behave like that observed for the PEO–NaSCN system in which a eutectic crystallization of a PEO–rich mixture takes place.

Experimental Section

Materials. The PEO sample (Dow Chemical Co., Polyglycol E-4000, lot number C-151) was purified by precipitation in petroleum ether from a 5% tetrahydrofuran solution and was subsequently dried at 70 °C under high vacuum. Its number-average molecular weight, M_n, determined by vapor pressure osmometry in benzene was $3.9 \pm 0.2 \times 10^3$ and its polydispersity index, M_w/M_n, characterized by gel permeation chromatography with ultrastyragel columns in tetrahydrofuran was 1.02. Anhydrous LiSCN was prepared after Lee[5] from the dihydrate $LiSCN\cdot(H_2O)_2$ (Pfaltz and Bauer, Inc.). For that purpose, first a 5% diethyl ether solution of the dihydrate dried under high vacuum at 60 °C was precipitated in petroleum ether. Then the precipitate, assumed by Lee[5] to be the etherate $LiSCN\cdot(C_2H_5)_2O$, was heated at 125 °C under high vacuum for a period of 24 h. This allowed the etherate decomposition to yield anhydrous LiSCN which, upon heating at 10 °C/min in the DSC apparatus, exhibited a single sharp endotherm at 284 °C. The characteristics of partially hydrated LiSCN were low-temperature endotherms at 49 and 67 °C and a dehydration broad endotherm in the range 140–200 °C followed by the LiSCN melting peak at 284 °C. NaSCN and KSCN purifications were described in the previous paper.[1] CsSCN (Pfaltz and Bauer, Inc.) was dried as-received by heating at 125 °C under high vacuum for a period of 24 h.

PEO–alkali thiocyanate mixtures of various compositions were prepared under dry atmosphere by mixing weighted quantities of 5% methanol solutions of each component and by evaporating methanol in a chamber flushed by dry nitrogen. The solid mixtures were subsequently dried for a week under high vacuum and stored in a glovebox. This last drying was performed at room temperature for all mixtures except those containing LiSCN. The latter were first heated at 125 °C for a period of 24 h. Methanol (Anachemia, reagent grade) was carefully dried before utilization.

DSC Measurement. Heating and cooling curves were recorded with a Model DSC-4 Perkin-Elmer calorimeter flushed with dry helium. Sample pans were filled and sealed under a dry atmosphere in a glovebox. Temperature calibrations were made by using standard materials with melting points in the range −39 to 327 °C. Energy calibrations were made by using the melting peak of indium recorded at 10 °C/min.

Conductivity Measurements. The samples were contained in a homemade cell consisting of two stainless steel solid cylinders encapsulated at both ends of a Teflon ring. A 1-cm diameter disk-shape electrode–electrolyte contact surface was imposed by the Teflon ring. The gap between the electrodes was 3.0 mm. For each sample, the latter was measured at room temperature with an accuracy better than 1% and no correction was made for the thermal expansion of the cell. The bulk electrolyte conductivity, σ, was measured by the ac complex impedance technique.[6] For that purpose, both the real part, Z', and the imaginary part, Z'', of the impedance of the cell were simultaneously recorded over the frequency range 5 Hz–13 MHz by using a Model 4192A Hewlett-Packard impedance analyzer.

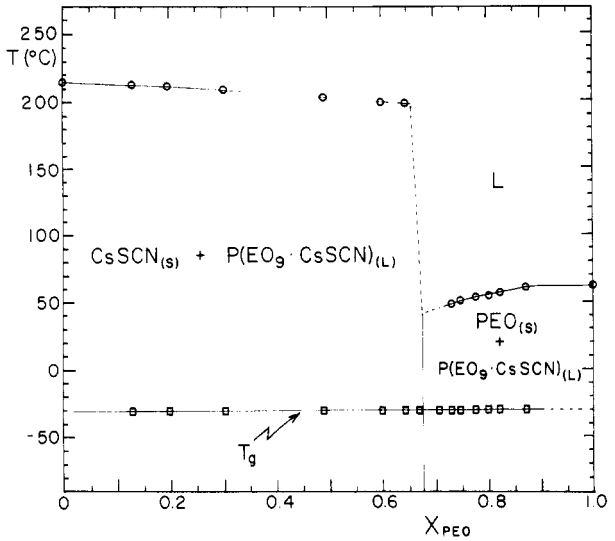

Figure 1. Temperature–composition diagram of the PEO–CsSCN system constructed by means of DSC measurements. The circles show the peak positions of the fusion endotherms recorded at 10 °C/min and the squares show the locations of the T_g's recorded at 40 °C/min, both for as-cast mixtures. The subscripts S and L denote crystalline and amorphous phases, respectively. The composition (X_{PEO}) is given in weight fraction of PEO.

The impedance data were collected by means of a Model 7090A Hewlett-Packard measurement plotting system that allowed the tracing of the familiar Z'' versus Z' complex impedance plot.[6] As usual, the bulk resistance of the electrolyte was assumed to correspond to the diameter of the high-frequency semicircle observed on the complex impedance plot.

The conductivity measurements were carried out at 5 °C intervals over various temperature ranges, depending upon the nature of the electrolyte. For that purpose, the cell was placed in a Model 3111 Instron temperature-controlled chamber. The temperature was measured with an accuracy better than ±0.5 °C by means of a digital thermometer whose probe was inserted in a well dug in the body of the cell Teflon ring.

Results and Discussion

Phase Diagram of the PEO–CsSCN System. Figure 1 shows a temperature–composition diagram constructed from the thermal events recorded by DSC upon heating a series of as-cast PEO–CsSCN mixtures having EO/Cs molar ratios ranging from 0.7 to 30. The composition is given in weight fraction of PEO designated by X_{PEO}. The diagram includes locations of melting endotherms (circles) recorded at 10 °C/min and also glass transition temperatures (squares) recorded at 40 °C/min. The former were measured at the peak maxima while the latter correspond to the intersection of the tangent drawn through the heat capacity jump with the base line measured before the glass transition.

It may be seen in Figure 1 that the phase diagram essentially consists of two nearly invariant melting equilibria that extrapolate to the melting points of the pure components (214 °C for CsSCN and 62 °C for PEO). Each of these equilibria corresponds to a specific domain of composition, indicating that the primitive system divides into two subsystems. In addition to the crystalline phases related to the foregoing melting equilibria, the system involves an amorphous phase of invariant composition that is present over the entire range of the mixture compositions. This is inferred from the observation of an invariant T_g located at −31 °C for all the as-cast mixtures. From the plot (shown in Figure 2) of the heat capacity increase per gram of sample, ΔC_p, at T_g as a function of X_{PEO}, it appears that the relative quantity of amorphous phase in the mixtures is maximum at the boundary of the two subsystems. Its composition at −31 °C, X^a_{PEO} (−31 °C), is close to 0.675 (EO/Cs = 9). Therefore, one of the subsystems consists of an amorphous phase of molar ratio EO/Cs = 9 saturated by CsSCN while the other consists of the same amorphous phase saturated by PEO.

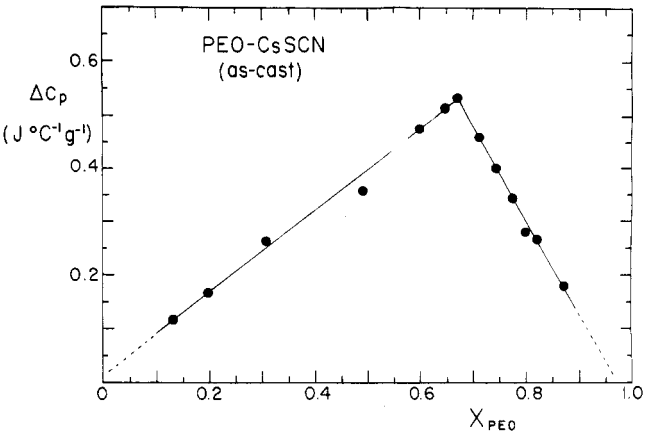

Figure 2. Variation with composition of the heat capacity increase per gram of sample, ΔC_p, at T_g (−31 °C) for the as-cast PEO–CsSCN mixtures.

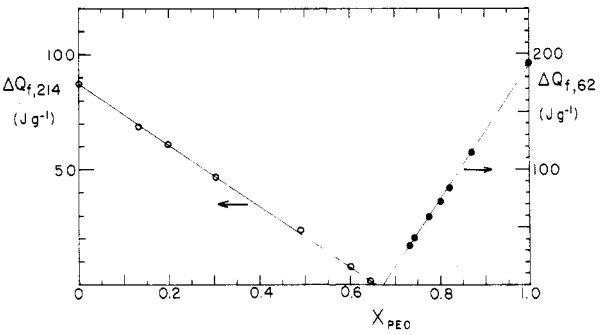

Figure 3. Variation with composition of the latent heats of fusion per gram of sample, $\Delta Q_{f,62}$ and $\Delta Q_{f,214}$, corresponding to the endotherms recorded near 62 °C and near 214 °C, respectively, both for the as-cast PEO–CsSCN mixtures.

The variation of X^a_{PEO} with temperature, that is the boundary of the two subsystems depicted by the dotted line in Figure 1, is nearly vertical. This boundary has been established by means of the calorimetric diagrams shown in Figure 3, in which the latent heats of fusion per gram of sample, $\Delta Q_{f,62}$ and $\Delta Q_{f,214}$, corresponding to the melting endotherms recorded near 62 and 214 °C, respectively, are plotted as a function of X_{PEO}. In either case the data points can be fitted by a straight line that extrapolates to the heat of fusion of the corresponding pure component. The composition-axis intercepts of these two lines characterize the composition of the amorphous phase near 62 and near 214 °C, respectively. The former is X^a_{PEO}(62 °C) = 0.675 identical to X^a_{PEO}(−31 °C) and the latter is X^a_{PEO}(214 °C) = 0.655, indicating a slight increase of salt solubility with increasing temperature from 62 to 214 °C.

Among the PEO–CsSCN mixtures investigated by DSC, there were two mixtures of compositions (X_{PEO} = 0.66 and 0.71) close to the boundary of the two subsystems. Although these mixtures did not exhibit any melting endotherm, their inspection by optical microscopy at room temperature revealed that the mixture with X_{PEO} = 0.66 contained CsSCN crystals while that with X_{PEO} = 0.71 contained crystalline PEO. This indicates that a sharp transition occurs upon change of composition near the boundary of the two subsystems. Such a sharp transition together with the invariance of X^a_{PEO}(−31 °C) with the global composition of the mixtures provides unambiguous evidence that a stoichiometric reaction takes place between

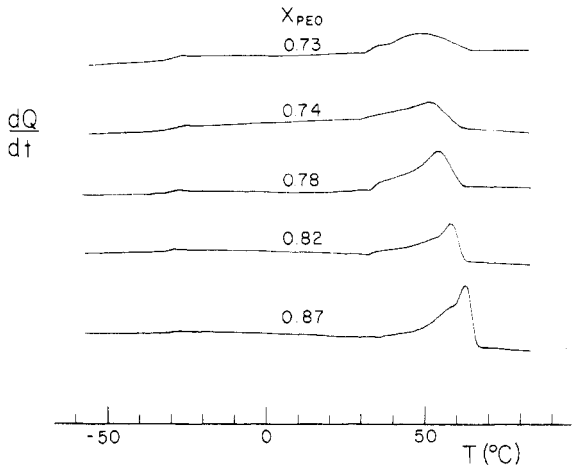

Figure 4. DSC heating curves recorded at 10 °C/min showing the progressive spreading, with decreasing PEO content, of the PEO fusion endotherms for PEO–CsSCN as-cast mixtures with X_{PEO} in the range 0.73–0.87.

PEO and CsSCN. On the other hand, the temperature independence of the boundary over a large domain of temperatures above T_g clearly indicates that CsSCN solubility in liquid PEO is governed by the same reaction. Therefore, the dissolution–solvation scheme previously proposed for the PEO–NaSCN and PEO–KSCN systems, that is the reaction scheme described by eq 1 and 2, also applies to the PEO–CsSCN system.

Another point which deserves mention concerns the thermal behavior of the mixtures belonging to the PEO-rich subsystem in the phase diagram of Figure 1; that is those characterized by a melting endotherm at a temperature near the melting temperature of PEO. Although this transition is reminiscent of the eutectic melt observed for many binary systems involving PEO and alkali metal salts,[1,7-10] it is fundamentally different. This point is particularly important because the composition of the eutectic mixture in most of these systems is close to the origin (X_{PEO} = 1), such that the existence of a true eutectic melt has been questioned in the literature.[11] For instance, for the PEO–NaSCN system characterized in the previous work[1] the eutectic composition is close to X_{PEO} = 0.93. The argument we gave for the presence of a true eutectic melt in this system was based upon the observation for all the mixtures having a PEO content greater than that of the P(EO_3·NaSCN) crystalline compound of a narrow melting endotherm that was invariant with a lowering of 4 °C with respect to the PEO endotherm at 62 °C. This argument was reinforced by the observation, when the same mixtures were melt recrystallized by slow cooling at 5 °C/min, of an invariant crystallization exotherm lying at a temperature 20 °C below that of the pure PEO sample at 42 °C.

In fact, as it may be seen in Figure 4, none of the as-cast PEO–CsSCN mixtures containing crystalline PEO show a narrow melting endotherm near 62 °C. They rather exhibit broad endotherms that become diffuse with increasing CsSCN content. On the other hand, as shown in Figure 5, when the same mixtures are melt recrystallized by slow cooling at 5 °C/min, they exhibit crystallization exotherms that move from 42 °C toward 10 °C with increasing CsSCN content. This latter behavior obviously results from the shortening of the uncomplexed EO unit sequences with decreasing PEO content of the melt. In turn, the spreading of the melting endotherms is a characteristic of crystalline lamellae of different thickness issued from EO unit sequences of different length.

Therefore, with respect to their crystallization behavior, the PEO–CsSCN mixtures belonging to the PEO-rich subsystem behave like random copolymers consisting of sequences of crystallizable and noncrystallizable units. The fact that PEO crystallization takes place without any evidence of redistribution of the complexed units in the liquid phase indicates that the latter are relatively stable. The situation appears to be completely different for eutectic crystallization such as that of the PEO–NaSCN system. In this case the formation of the crystalline compound takes place through a reaction that builds up long sequences of EO_3·NaSCN units and thereby contributes to the formation of long sequences of uncomplexed EO units. Since the eutectic composition is rich in PEO, these sequences are probably long enough to crystallize in the form of crystallites of even thickness that exhibit narrow melting.

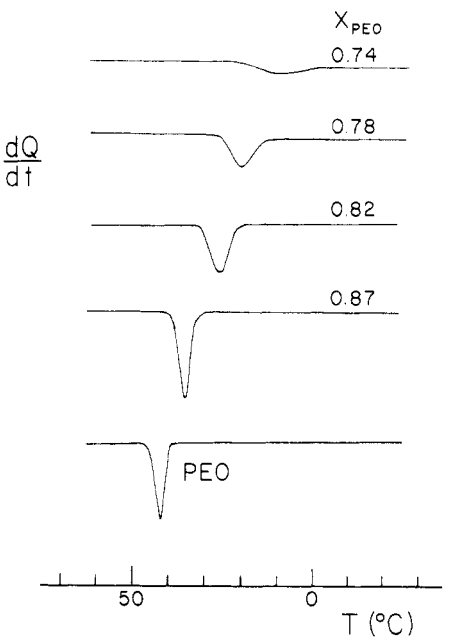

Figure 5. DSC cooling curves recorded at 5 °C/min showing the temperature lowering, with decreasing PEO content, of the PEO crystallization exotherms for PEO–CsSCN mixtures with X_{PEO} in the range 0.74–1. Curves recorded from the melt after a heating for a period of 15 min at 80 °C.

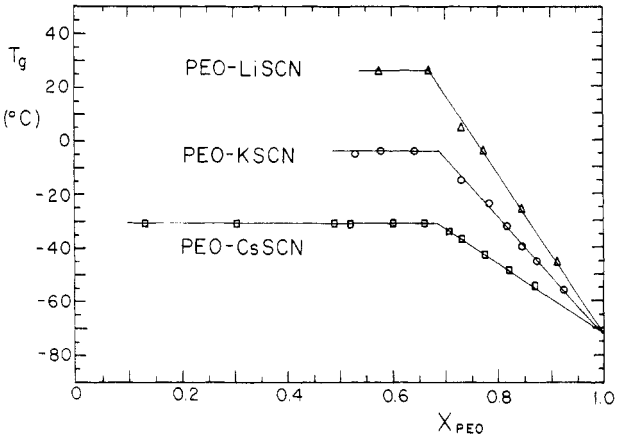

Figure 6. Variation of T_g with PEO weight fraction for supercooled PEO–LiSCN, PEO–KSCN, and PEO–CsSCN mixtures. Prior to T_g measurements all mixtures were melt-quenched by a rapid cooling to −100 °C at 320 °C/min in the DSC apparatus.

Thermal Properties and Structural Features of Supercooled PEO–Alkali Thiocyanate Mixtures. Figure 6 shows plots of T_g as a function of PEO weight fraction for supercooled PEO–LiSCN, PEO–KSCN, and PEO–CsSCN mixtures obtained by rapid cooling (320 °C/min) in the DSC apparatus. Each plot exhibits the

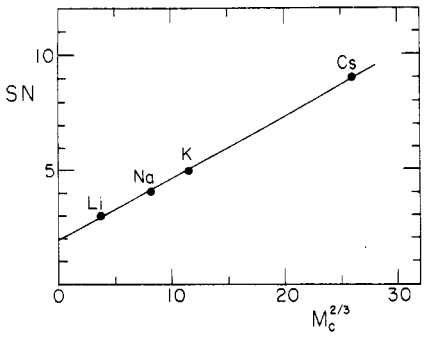

Figure 7. Plot of the apparent solvation numbers, SN, of the various alkali thiocyanates as a function of the cation atomic weights, M_c, to the power $^2/_3$.

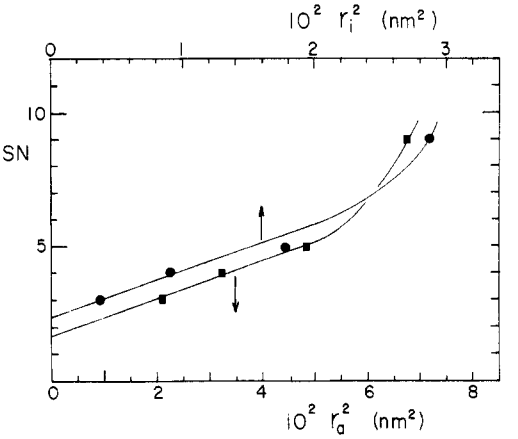

Figure 8. Plots of the apparent solvation numbers, SN, of the various alkali thiocyanates as a function of the square of the ionic radii (r_i, after Pauling and Sherman[12]) and the square of the atomic radii (r_a, after Slater[13]) of the corresponding alkali metals.

same general features. With increasing X_{PEO}, T_g first remains invariant at a temperature which is an inverse function of the cation size, and then at about the same value of X_{PEO}, close to 0.68, it linearly decreases to extrapolate to the same value close to −72 °C at zero salt content (X_{PEO} = 1). The intersection between the horizontal and inclined segments of each curve provides a characterization for the solubility of each salt in amorphous PEO at the corresponding T_g. When expressed on a molar ratio basis, LiSCN, KSCN, and CsSCN solubilities correspond to EO/Li = 3, EO/K = 4.9, and EO/Cs = 9, respectively. The PEO–NaSCN system is not shown in Figure 6 because salt-saturated supercooled mixtures are impossible to obtain with NaSCN. Indeed, an important crystallization of the P(EO_3·NaSCN) compound occurs even upon quenching at 320 °C/min.[1]

Assuming that LiSCN solubility is governed by a dissolution–solvation scheme similar to that previously established for the other alkali thiocyanates, each of these three EO/M ratios, together with the ratio EO/Na = 4 (X_{PEO} = 0.68) previously established for NaSCN solubility at temperatures just above the melting point of P(EO_3·NaSCN), would correspond to the stoichiometry of the solvate formed for each salt according to eq 2. The fact that these ratios, thereafter designated as the apparent solvation numbers, SN, of the salts, correspond to about the same PEO weight fraction close to 0.68 suggests that solvation of alkali thiocyanates is governed by a simple geometric factor related to the cation size. This geometric factor appears to be the cation surface. Indeed, as shown in Figure 7, a plot of SN as a function of the cation atomic weight, M_c, to the power $^2/_3$, a quantity expected to be roughly proportional to the cation spherical surface, yields a linear curve which extrapolates to SN = 2 at a zero value of M_c. Similar behavior is observed in Figure 8 where SN is plotted as a function of both the square of the ionic radius and the square of the atomic radius of each alkali metal. These two latter sets of empirical radius data[12,13] should more adequately represent the extremal values for the cation spherical surface. Though not perfectly linear, either of these plots also extrapolates to a finite value of SN close to 2 at a zero radius value.

When recent data for NaI and $NaB(Ph)_4$ are compared to the present data for NaSCN, it may be seen that the anion size also plays an important role on the solvate stoichiometry. Indeed, in a paper[10] devoted to the PEO–NaI system, a partial phase diagram is reported that indicates a solvation number of 6 for NaI, while a phase diagram constructed in our laboratory for the PEO–$NaB(Ph)_4$ system[14] indicates a solvation number of 8 for $NaB(Ph)_4$. Like the present SN value of 4 for NaSCN, both these SN values of 6 and 8 are indicated by salt solubility data at temperatures just above the incongruent melting of the corresponding intermediate compounds P(EO_3·NaI) and P(EO_5·$NaB(Ph)_4$), respectively. These preliminary data concerning sodium salts also reveal a nearly linear correlation (not shown) between SN and anion formula weight, M_a, to the power $^2/_3$. A least-squares fitting of the corresponding three data points yields an intercept close to SN = 2.5 at a zero value of M_a. Interestingly, the sum of this result with the former result (SN = 2 at a zero value of M_c for the thiocyanates), that is the sum of the apparent quantities $SN(Na^+)$ and $SN(SCN^-)$ expected to be given by the intercepts, nearly coincides with the apparent solvation number (SN = 4) previously characterized for NaSCN. This agreement might be fortuitous, but it might also indicate that the SN value established for each alkali thiocyanate could be the sum of two independent variables: an apparent solvation number of value close to 2 for the thiocyanate ion and an apparent coordination number of value close to SN − 2 for the alkali ion.

This simple model concerning solvation of alkali-metal salts is purely hypothetical. Nevertheless, as will be shown in the next section, it provides a coherent framework for rationalizing cation size effect upon the conductivity magnitude of PEO–alkali thiocyanate amorphous mixtures. The apparent solvation number SN inferred from the solubility data on the basis of the present dissolution–solvation scheme is necessarily related to a state of minimum energy resulting from a balance of several forces including ion–ion Coulombic interactions, ion–dipole interactions (cation coordination), and dipole–dipole interactions (anion solvation). In this respect, the apparent coordination number SN − 2 might be a real feature of the cation, namely, its actual coordination number in terms of EO units, but the apparent solvation number of 2 for the thiocyanate ion might rather correspond to the minimum number of additional EO units necessary to stabilize the whole solvate structure. Also, it is likely that an exchange of these two types of EO units could occur at a rate that is an inverse function of the cation coordination binding energy. Unfortunately, the present data deduced of calorimetric measurements cannot provide any direct evidence for such structural features. Only spectroscopic techniques capable of probing the structural features at a rate greater than the exchange rate could possibly clarify this question.

In order to examine in more detail the effect of cation size upon segmental motion, particularly in the subsaturated domain of concentration where an important amount of EO units should be outside the solvation shells of the

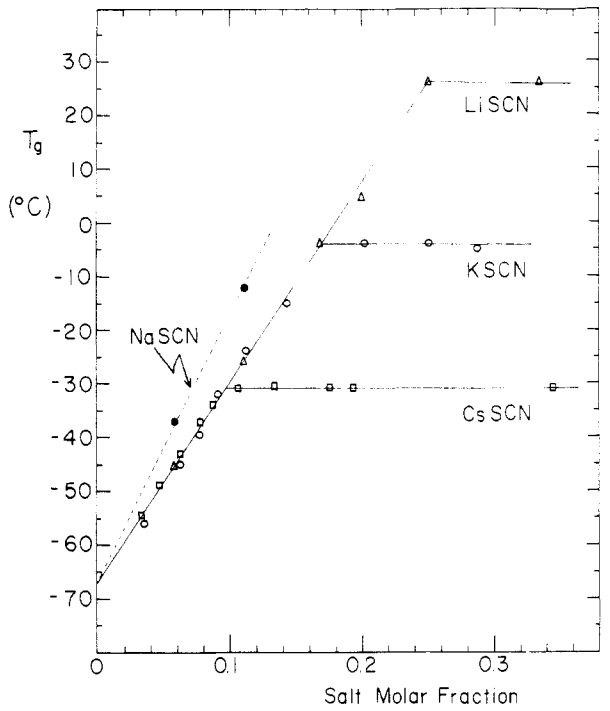

Figure 9. Variation of T_g with salt molar fraction for supercooled PEO–LiSCN, PEO–NaSCN, PEO–KSCN, and PEO–CsSCN mixtures. Same data as in Figure 6 with the addition of the two data points for PEO–NaSCN mixtures.

ionic species, the T_g data of Figure 6 are plotted as a function of the salt molar fraction in Figure 9. Also plotted in Figure 9 are two data points not shown in Figure 6, corresponding to PEO–NaSCN unsaturated mixtures that were successfully quenched under the form of completely amorphous materials.[1] This new representation of the T_g data reveals that all the alkali thiocyanates except NaSCN produce essentially the same linear T_g elevation close to 4 °C per mol % of salt, while NaSCN yields a larger T_g elevation close to 5 °C per mol %. Note that the present T_g data for NaSCN are identical with recent data reported for melt-quenched PEO–NaSCN mixtures made with a high molecular weight (6×10^5) PEO sample.[9] Interestingly, nearly identical data were also quoted for PEO–NaI mixtures made with the same PEO sample.[15] On the other hand, some T_g data[11] reported for PEO–$LiCF_3SO_3$ mixtures also made with a high molecular weight PEO sample appear to coincide with the present data for LiSCN, KSCN, and CsSCN.

This comparison of T_g elevation for a limited number of PEO–alkali salt systems seems to indicate that segmental motion is nearly independent of either cation or anion size except for a specific effect associated with the sodium cation. This independence of T_g upon ion size is puzzling, particularly if one considers that the ion size appears to have an important effect upon solvation properties as indicated in the foregoing analysis of solubility data. In order to be coherent with this analysis we are forced to consider that a balance of effects should occur for yielding such a behavior, otherwise serious doubts should be cast upon the relevance of the foregoing interpretation. By taking into consideration that it is probably cation coordination with its large binding energy that is the main source of perturbation for chain motion, the resulting T_g elevation should depend upon both the fraction of EO units directly bound to the cations and the average binding energy for these units. Since a large cation such as Cs^+ (having a large apparent coordination number) is characterized by a smaller surface charge density than a small cation such as Li^+ (having a small apparent coordination number), the same T_g elevation for these two cations (and also for K^+) might result from a nearly perfect balance of coordination number effect and binding energy effect. In other words, binding energy would be inversely proportional to the cation apparent coordination number. This explanation is purely hypothetical and only further investigation dealing with the dynamics of the present systems could really clarify this point. If this explanation is correct, it is not impossible that the larger T_g elevation observed for the sodium salts could result from a greater binding energy associated with a local conformation of the PEO chain that would better fit the size of sodium cation than that of the other cations.

Solvation Effect on Conductivity of Concentrated Amorphous Mixtures. It is well documented that ionic conduction in semicrystalline PEO electrolytes occurs within their amorphous regions and that conductivity, σ, of the latter, as well as that of completely amorphous electrolytes made with PEO or PEO-containing polymers, is closely related to the polymer chain dynamics.[2-4] This is indicated by a temperature dependence of σ in agreement with well-known empirical equations previously established for the temperature dependence of rheological properties of amorphous polymers at temperatures above T_g. Among these equations are the Vogel–Tammann–Fulcher (VTF) equation for viscosity, and the Williams–Landel–Ferry (WLF) equation for viscoelastic properties.

Conductivity data for various PEO amorphous electrolytes have been successfully fitted by an adjustable three-parameter equation of the form[2,16]

$$\sigma(T) = A \exp[-B/(T - T_\infty)] \quad (3)$$

similar to the VTF equation for viscosity[17]

$$\eta(T) = A' \exp[B'/(T - T_\infty)] \quad (4)$$

in which T_∞ is the temperature at which η becomes infinite and B' is a constant assumed to be a characteristic of the polymer chain stiffness. Note that both eq 3 and 4 are often written with a preexponential phenomenological factor, A or A', assumed to vary as $T^{-1/2}$. However, this $T^{-1/2}$ variation is of little effect when compared to that associated with the exponential term.

The WLF equation for viscoelastic properties (relaxation moduli or creep compliances) may be considered as a more general form of the VTF equation. It is an adjustable two-parameter equation that gives the temperature dependence of the shift factor a_T for the time–temperature superposition of viscoelastic properties. Basically, this factor corresponds to the ratio $\tau(T)/\tau(T_0)$ of any mechanical relaxation time (or retardation time) at temperature T to its value at a reference temperature T_0. For relaxation times, which are quantities that decrease with increasing temperature, the WLF equation is written as follows[17]

$$\ln \tau(T)/\tau(T_0) = -C_1(T - T_0)/[C_2 + (T - T_0)] \quad (5)$$

where C_1 and C_2 are positive constants characteristic of both the nature of the polymer and the reference temperature T_0.

An important feature of eq 5 is its nearly universal character. Indeed, when it is fitted to the relaxation data of different polymers by using for each of them a reduced T_0 value such that $T_0 - T_g$ equals a constant, it often yields about the same values for the adjustable parameters C_1 and C_2.[17]

By assuming that η and τ exhibit the same temperature dependence, it may be shown that the parameters C_1 and C_2 of the WLF equation are related to the parameters B'

and T_∞ of the VTF equation as follows:

$$C_1 = B'/(T_0 - T_\infty) \quad (6)$$

$$C_2 = T_0 - T_\infty \quad (7)$$

Therefore, it may not be surprising that an analytical expression similar to the WLF equation involving the variable $\ln \sigma(T_0)/\sigma(T)$ instead of $\ln \tau(T)/\tau(T_0)$ can fit conductivity data as well as eq 3 similar to the VTF equation for viscosity. Such fittings based upon the WLF equation have been successfully applied to conductivity data of completely amorphous electrolytes made with PEO or poly(propylene oxide) (PPO) polyurethane networks.[3,4] The great merit of this latter approach was to reveal that the C_1 and C_2 parameters deduced from conductivity data exhibit a great similarity to those deduced from mechanical relaxation data for the same materials.[3] This indicates a direct correlation between ionic mobility and polymer chain motion, but the reason for such a correlation is not clear.

The main difficulty encountered in the analysis of conductivity data related to polymer electrolytes is the lack of a microscopic model that could be used for a tentative interpretation, if only for testing a well-defined hypothesis. Indeed, some fundamental aspects such as the nature of the ionic species and their transportation mechanism through the polymer lattice are still discussed at a very speculative level.[18] However, there are a number of reported experimental data and interpretations that suggest some guidelines for attacking this problem.

First, in solvents of low dielectric constant such as PEO and PEO-containing polymers, ion pairing and multiplet formation take place at relatively low salt concentrations. This is indicated by the concentration dependence of the molal conductivity, $\Lambda = \sigma/m$ (m = salt molality), reported for various electrolytes in the regime of the very low and moderate concentrations.[19,20] With increasing m, Λ first decreases abruptly, passes through a minimum for m values in the vicinity of 0.02 mol/kg (EO/M close to 1000), and exhibits a further rise above this concentration. A quantitative analysis of such Λ data for $LiClO_4$ and $LiCF_3SO_3$ dissolved in a liquid PEO (M_n = 400) was reported[19] in which an interpretation is made in terms of a model involving ion pairs in equilibrium with a decreasing amount of free ions and an increasing amount of triplets with increasing salt concentration. According to this interpretation, at concentrations as low as 0.1 mol/kg (EO/M $\simeq$ 230) less than about 5% of the salt would be under the form of free ions while more than 30% of it would be under the form of triplets. Very similar behavior was also reported for alkali thiocyanates dissolved in a liquid copolymer of ethylene oxide with propylene oxide.[20] At higher salt concentrations, that is for EO/M less than about 50, the T_g change with concentration becomes important and the conductivity data are no longer interpretable in terms of the concentration dependence of Λ at a given temperature. Indeed, for many systems[20-22] either σ or Λ exhibits a maximum at salt concentrations corresponding to EO/M molar ratios in the range 20–25, a behavior which is partly due to the increase of T_g with increasing salt content. Therefore, any analysis in terms of concentration or ion size effect in the concentrated regime should be made after an appropriate separation of the T_g effect upon conductivity. This is usually done by comparing the data at the same reduced temperature $T - T_g$.

Second, the VTF or WLF behavior for the temperature dependence of σ suggests a conduction mechanism in which the charged species are allowed to migrate through the polymer lattice owing to the segmental motion of the latter. Since such a motion does not involve long-range translation, the migration might occur by a hopping-type process through exchange of EO solvating units.[18,23] If that is the case, conduction should be governed by ion–dipole interactions (cation coordination) in addition to segmental motion and ion–ion interactions. The interpretation given in the preceding sections of the solubility behavior in terms of a predominant effect related to ion–dipole interactions necessarily reinforces this view that the latter might also be a basic parameter for conduction. Indeed, any parameter governing the stabilization of the ionic structure, as is apparently the case for the ion–dipole interactions, should be a fundamental parameter in the conduction mechanism.

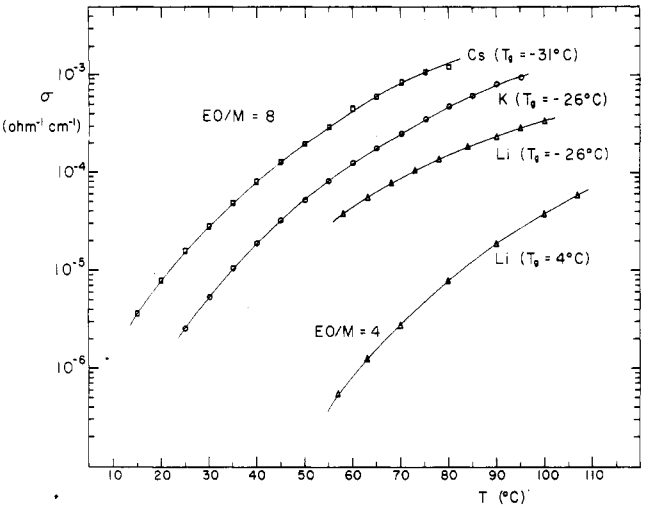

Figure 10. Semilogarithmic plots of conductivity σ as a function of temperature for EO/M = 8 PEO–LiSCN, PEO–KSCN, and PEO–CsSCN amorphous mixtures and for an EO/M = 4 PEO–LiSCN amorphous mixture. The EO/Cs = 8 mixture was saturated by a slight amount of CsSCN. The actual composition of its amorphous phase was EO/Cs = 9.

On the basis of the phase diagrams of the present PEO–alkali thiocyanate systems, it has been possible to define a common EO/M ratio for which three of these systems yield complete or near complete amorphous mixtures suitable for a conductivity study. This ratio is EO/M = 8. For LiSCN, it corresponds to a mixture in which a small amount of crystalline PEO is present, but only for temperatures below 60 °C. For KSCN this composition yields a noncrystallizable mixture while for CsSCN it yields an amorphous mixture saturated by a slight amount of salt. The real composition of the polymeric phase in the latter mixture is EO/Cs = 9. NaSCN was excluded for the reasons given in the foregoing section.

In addition to these three mixtures, a second PEO–LiSCN mixture having an EO/Li ratio of 4 was investigated. This mixture was noncrystallizable. It allowed us to examine the effect of concentration upon the conductivity of one of the polymer electrolytes, all of them being prepared with the same 4×10^3 molecular weight PEO sample. At room temperature, the EO/M = 8 mixtures of low T_g's (−31 to −26 °C) were viscous materials while the EO/Li = 4 mixture of higher T_g (4 °C) was an elastomeric material.

Figure 10 shows semilogarithmic plots of the conductivity data as a function of temperature. The three upper plots correspond to the nominal EO/M = 8 mixtures while the lower plot corresponds to the EO/Li = 4 mixture. The data of both the EO/Li = 4 and EO/Li = 8 mixtures are limited to temperatures above 60 °C, because below this limit the former exhibited conductivities lower than 1 ×

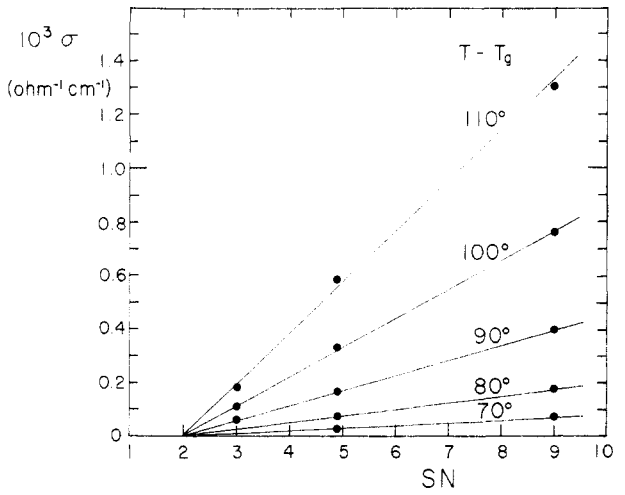

Figure 11. Diagram showing the linear correlation between the conductivity data at constant values of $T - T_g$ and the apparent solvation numbers, SN, for LiSCN (3), KSCN (4.9), and CsSCN (9). Based on the conductivity data shown in Figure 10 for the EO/M = 8 mixtures.

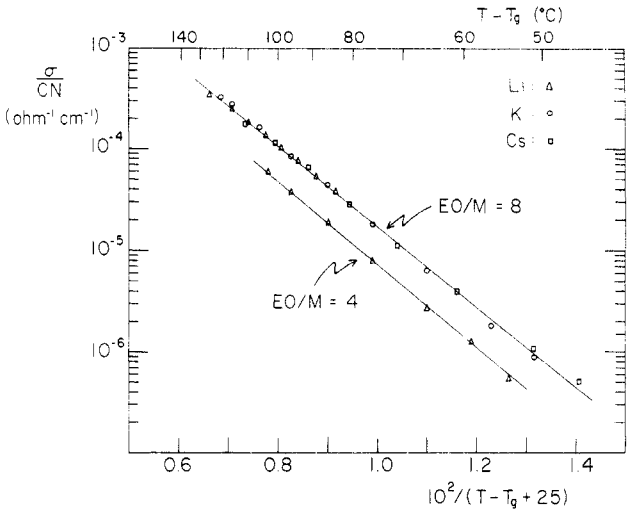

Figure 12. Semilogarithmic plots, according to eq 3, of σ/CN as a function of $(T - T_g + 25)^{-1}$. In these plots, based on the conductivity data shown in Figure 10, CN is the apparent coordination number for the cation (1 for Li^+, 2.9 for K^+, and 7 for Cs^+), a constant applied to the denominator of both sides of eq 3. The variable $(T - T_g + 25)$ corresponds to the variable $(T - T_\infty)$ of eq 3 in which T_∞ is adjusted to the quantity $(T_g - 25)$ that gives the best linear fit of the whole data.

10^{-7} Ω^{-1} cm^{-1} that were difficult to measure with accuracy and the latter contained some crystalline PEO as previously mentioned. As already documented in the literature for similar electrolytes made with various PEO-containing polymers,[20-22] at a given molar ratio EO/M, conductivity decreases markedly with decreasing alkali-metal cation size.

As a first step in the present data analysis, it was imperative to examine whether a correlation exists between the conductivity magnitude of the EO/M = 8 mixtures made with LiSCN, KSCN, and CsSCN and the apparent solvation number, SN, previously characterized for each of these salts. Such an analysis is depicted in Figure 11, in which plots as a function of SN of the conductivity data at constant values of $T - T_g$ are shown for different values of $T - T_g$ ranging from 70 to 110 °C. Surprisingly, each plot is linear and exhibits the same intercept close to SN = 2, indicating that the conductivity magnitude at a given value of $T - T_g$ is directly proportional to the quantity SN − 2. Note that according to the interpretation given in the preceding section, this latter quantity should correspond to the apparent coordination number characteristic of each cation, that is CN = 1 for Li^+, CN = 2.9 for K^+, and CN = 7 for Cs^+.

In order to examine in more detail the range of validity of the above correlation, the whole conductivity data were analyzed according to eq 3 based upon the VTF approach. For this analysis, the parameter A in eq 3 was assumed to be proportional to CN and linear least-squares fits of plots of ln σ/CN as a function of $(T - T_g + \Delta T)^{-1}$ were made for each electrolyte for values of ΔT incremented by steps of 5 °C over the range ΔT = 0–100 °C. The best fits were obtained for ΔT = 25 °C, that is for $T_\infty = (T_g - 25)$ in eq 3. As shown in Figure 12, this adjustment for T_∞ yields a single composite curve for the three EO/M = 8 electrolytes, this curve being characterized by a B parameter equal to 9.1×10^2 and a pre-exponential factor A/CN equal to 0.157 Ω^{-1} cm^{-1}. In turn, the data for the EO/Li = 4 electrolyte fall on a second curve which is nearly parallel to the first but shifted to lower σ/CN values. This second curve is characterized by a B parameter equal to 9.5×10^2 and a preexponential factor A/CN equal to 0.094 Ω^{-1} cm^{-1}. Interestingly, the present B values in the range $(9.1–9.5) \times 10^2$ are nearly identical to B' values in the range $(8.1–9.3) \times 10^2$ previously reported for low molecular weight $(9 \times 10^2–2 \times 10^4)$ pure PEO. These B' values, as well as $T_\infty = (T_g - 26) \pm 2$ close to the present T_∞ value, were quoted as the best VTF parameters for the PEO viscosity data in the temperature range 70–140 °C.[24]

It thus appears that the temperature dependence of σ for the present electrolytes is identical with that of η for pure PEO. Therefore, it is the assumed temperature-independent preexponential factor A in eq 3 that mainly accounts for the change of conductivity associated with either the nature of the salt or its concentration in the system. Note that this behavior was already expected on the basis of a previous work made on PEO and PPO polyurethane networks for which the WLF C_1 and C_2 parameters deduced from conductivity data for $NaB(Ph)_4$ were shown to be nearly identical with those deduced from relaxation modulus data for salt-free systems.[3] The WLF parameters computed from the present B and T_∞ data by means of eq 6 and 7 are C_1 = 37 (natural logarithm) and C_2 = 25 °C, respectively, for a reference temperature T_0 in eq 5 adjusted to T_g. Only the former is in close agreement with the pseudouniversal values quoted for these parameters, that is C_1 = 40 (natural logarithm) and C_2 = 52 °C, respectively.[17]

From the perfectly superimposed plots of the EO/M = 8 composite data in Figure 12, it may be inferred that σ is directly proportional to CN over the entire 85 °C range of the variable $T - T_g$ covered in the present study. At first glance, this behavior suggests that it is the same type of interactions that govern both solvate formation and conduction mechanism. These interactions apparently yield an ionic structure that, at a given reduced temperature $T - T_g$, can release an amount of charge carriers proportional to the apparent coordination number of the cation. On the other hand, the nearly invariant B parameter in eq 3, together with its value close to that of the B' parameter in eq 4 for pure PEO, seems to indicate that the activation energy for the charge carrier formation is negligible with respect to that related to the chain motion.

A tentative explanation for such behavior cannot be made without some speculations concerning the ionic structure of the present electrolytes. If, according to the view often proposed for concentrated polyether electrolytes, the charge carriers were free ions or odd-numbered multiplets in equilibrium with ion pairs or even-numbered

multiplets, their concentration would be governed by ion–ion interactions and would presumably increase with temperature according to an Arrhenius behavior characterized by a nonnegligible activation energy. A structure that would be more consistent with the present data might rather consist of solvated ions distributed in the same manner as in an ionic crystalline substance, that is, ions surrounded by an ion atmosphere of opposite sign. Upon thermal motion, the ions would undergo a change of position through either exchange of solvating EO units (for the cations) or diffusion (for the anions). These random fluctuations would occur with a continuous rearrangement of the ion atmosphere, that is, with a concomitant displacement or exchange of neighboring ions. An external field applied to such a system would impose a small directional component on the random fluctuations and the net effect would be a mobility for the ions that would exhibit a temperature dependence governed by thermal motion only.

The present model would not only account for the apparent negligible activation energy related to charge carrier formation but it would also provide a rational framework for a tentative interpretation of the correlation between σ and CN. Indeed, according to this model, at a given molar ratio EO/M in the concentrated regime, the average distance between ions would be the same for the three thiocyanates. Since the ion–ion interaction effect upon ion mobility is expected to depend upon this average distance, it would turn out that this effect could be the same for the three EO/M = 8 electrolytes. If that is really the case, the correlation between σ and CN might be interpreted in terms of solvation effect only. On this ground, and by considering the hypothesis made in the preceding section that the cation–EO binding energy would be inversely proportional to CN for these three electrolytes, the linear increase of σ with CN might be interpreted in terms of a decrease of binding energy with increasing cation size. This view is not unreasonable, since it is expected that the rate of exchange of EO units upon thermal motion should be an inverse function of the cation–EO binding energy.

A last remark concerns the effect of salt concentration in the regime close to saturation. The VTF plots shown in Figure 12 for the mixtures with EO/Li ratios of 8 and 4 indicate that a 2-fold increase of salt concentration yields about a 2-fold decrease of σ, this at constant value of $T - T_g$ and over all the 85 °C range of this last variable. In terms of the present model, two factors could be at the origin of this effect: first the stronger ion–ion interactions resulting from the closer average distance between ions and second the fewer number of free EO units available for the hopping process. Obviously, further studies are required in order to clarify this question. Of particular importance would be to investigate the effect of salt concentration for the other alkali thiocyanates and to examine the relation between σ an CN over a wider range of concentrations below the saturation conditions.

Acknowledgment. This work was supported by the Quebec Ministry of Education and by the Research Institute of Hydro-Quebec. S.B. wishes to thank the Xerox Research Centre of Canada for having received the 1987 Xerox Fellowship in Chemistry and Chemical Engineering.

References and Notes

(1) Robitaille, C.; Marques, S.; Boils, D.; Prud'homme, J. *Macromolecules* **1987**, *20*, 3023.
(2) Armand, M. *Solid State Ionics* **1983**, *9–10*, 745.
(3) Killis, A.; Le Nest, J. F.; Gandini, A.; Cheradame, H.; Cohen-Addad, J. P. *Solid State Ionics* **1984**, *14*, 231.
(4) Watanabe, M.; Itoh, M.; Sanui, K.; Ogata, N. *Macromolecules* **1987**, *20*, 569.
(5) Lee, D. A. *J. Inorg. Chem.* **1964**, *3*, 289.
(6) Bruce, P. G. In *Polymer Electrolyte Reviews—1*; MacCallum, J. R., Vincent, C. A., Eds.; Elsevier Applied Science: New York, 1987; p 237.
(7) Stainer, M.; Hardy, L. C.; Whitmore, D. H.; Shriver, D. F. *J. Electrochem. Soc.* **1984**, *131*, 784.
(8) Robitaille, C.; Fauteux, D. *J. Electrochem. Soc.* **1986**, *133*, 315.
(9) Lee, Y. L.; Crist, B. *J. Appl. Phys.* **1986**, *60*, 2683.
(10) Fauteux, D.; Lupien, M. D.; Robitaille, C. *J. Electrochem. Soc.* **1987**, *134*, 2761.
(11) Minier, M.; Berthier, C.; Gorecki, W. *J. Chim. Phys.* **1984**, *45*, 739.
(12) Pauling, L.; Sherman, J. *Z. Krist.* **1932**, *81*, 1.
(13) Slater, J. C. *J. Chem. Phys.* **1964**, *41*, 3199.
(14) Vallée, A.; Prud'homme, J., unpublished results.
(15) Lee, Y. L. Ph.D. Thesis, Northwestern University, 1987.
(16) Armand, M. B. In *Polymer Electrolyte Reviews—1*; MacCallum, J. R., Vincent, C. A., Eds.; Elsevier Applied Science: New York, 1987; p 1.
(17) Ferry, J. D. *Viscoelastic Properties of Polymers*; John Wiley: New York, 1980; Chapter 11.
(18) Ratner, M. A. In *Polymer Electrolyte Reviews—1*; MacCallum, J. R., Vincent, C. A., Eds.; Elsevier Applied Science: New York, 1987; p 173.
(19) MacCallum, J. R.; Tomlin, A. S.; Vincent, C. A. *Eur. Polym. J.* **1986**, *22*, 787.
(20) Cameron, G. G.; Harvie, J. L.; Ingram, M. D.; Sorrie, G. A. *Br. Polym. J.* **1988**, *20*, 199.
(21) Tada, H.; Fujino, K.; Kawahara, H. *J. Polym. Sci., Polym. Chem. Ed.* **1987**, *25*, 3015.
(22) Watanabe, M.; Ikeda, J.; Shinohara, I. *Polym. J.* **1983**, *15*, 175.
(23) Papke, B. L.; Ratner, M. A.; Shriver, D. F. *J. Electrochem. Soc.* **1982**, *129*, 1694.
(24) Privalko, V. P.; Lipatov, Yu. S.; Lobodina, A. P.; Shumskii, V. F. *Polym. Sci. USSR (Engl. Transl.)* **1974**, *16*, 3229.